



**HAL**  
open science

## Upgrading wave energy test sites by including overplanting: a techno-economic analysis

Anne Blavette, Charles-henri Bonnard, Ildar Daminov, Salvy Bourguet,  
Thomas Soulard

### ► To cite this version:

Anne Blavette, Charles-henri Bonnard, Ildar Daminov, Salvy Bourguet, Thomas Soulard. Upgrading wave energy test sites by including overplanting: a techno-economic analysis. *IET Renewable Power Generation*, 2021, 10.1049/rpg2.12220 . hal-03246886

**HAL Id: hal-03246886**


**<https://hal.science/hal-03246886>**

Submitted on 2 Jun 2021

**HAL** is a multi-disciplinary open access archive for the deposit and dissemination of scientific research documents, whether they are published or not. The documents may come from teaching and research institutions in France or abroad, or from public or private research centers.

L'archive ouverte pluridisciplinaire **HAL**, est destinée au dépôt et à la diffusion de documents scientifiques de niveau recherche, publiés ou non, émanant des établissements d'enseignement et de recherche français ou étrangers, des laboratoires publics ou privés.

# Upgrading wave energy test sites by including overplanting: a techno-economic analysis

Anne Blavette<sup>1</sup>  | Charles-Henri Bonnard<sup>1,2</sup> | Ildar Daminov<sup>1,2</sup> | Salvy Bourguet<sup>2</sup> | Thomas Soulard<sup>3</sup>

<sup>1</sup> Univ. Rennes, ENS Rennes, CNRS, SATIE lab, avenue R. Schuman, Bruz, France

<sup>2</sup> IREENA, University of Nantes, 37 Boulevard de l'Université, BP 406, Saint-Nazaire, Cedex, France

<sup>3</sup> LHEEA, École Centrale de Nantes, 1 Rue de la Noë, Nantes, France

## Correspondence

Anne Blavette, Univ. Rennes, ENS Rennes, CNRS, SATIE lab, avenue R. Schuman, 35170 Bruz, France.  
[Anne.Blavette@ENS-Rennes.fr](mailto:Anne.Blavette@ENS-Rennes.fr)

## Funding information

CARENE; WEAMEC; Ecole Normale Supérieure de Rennes; Conseil Régional de Bretagne, Grant/Award Number: SAD17021; Conseil Régional des Pays de la Loire

## Abstract

Dynamic rating is an approach which implies to operate an electrical network closer to its thermal limits. This approach may be very beneficial for wave farms, as they are expected to present a highly fluctuating electrical current profile while benefiting from the large thermal inertia of the soil where their export cable will be buried. However, as the implementation of this approach is still in its infancy for offshore wind farms, it may be expected that the first wave farms, under the form of small-scale test sites, will be sized with respect to electrical current limits at a first stage. This sizing may be upgraded at a second stage when design methods will have included dynamic rating. However, this raises the question of the economic feasibility of this two-step approach, which is studied in this paper. Also, performing such a techno-economic analysis requires developing an electrothermal model of the export cable able to represent its transient response in a sufficiently precise manner while requiring also a reasonable computing time. In this perspective, a comparative analysis between several electrothermal modelling methods is also described in this paper.

## 1 | INTRODUCTION

The electricity sector is to become more and more sustainable. This will be achieved through various ways, such as by integrating more and more renewable energies into the grid, but also by minimizing the use of natural resources necessary for electrical systems, for example in maximising the use of already existing infrastructures [1]. This emerging trend in distribution and transmission system operators will lead to their systems being operated increasingly closer to the infrastructure technical limits. In particular, cables are expected to be operated closer to their maximum allowed temperature which constitutes the limiting factor. Such an approach can postpone, or even prevent, time-consuming and costly grid reinforcements. In this perspective, the so-called “dynamic rating” approach is progressively being adopted by grid operators and applied primarily to overhead lines (hence the term “dynamic line rating”) [2], although it is envisaged to be applied to transformers as well [3, 4]. In this concept, the maximum current allowed for a piece of equipment is adjusted dynamically with the ambient conditions (including ambient temperature, solar radiation level, wind speed, etc.).

For underground or submarine cables, ambient conditions are relatively stable with time. However, the large thermal inertia provided mostly by the soil allows to apply dynamic rating as well. Under these conditions, a current greater than the steady-state, rated current can be applied on a temporary basis on the cable without its temperature exceeding its maximum allowed limit. Exploiting this thermal inertia may allow to design cables for a rated current below the maximum current they would have to transmit, therefore reducing the need for natural resources. It may also allow to increase the maximum level of current an existing cable may transmit, thus increasing the use of existing infrastructures. Some works have investigated dynamic cable rating applied to offshore wind farms and the resulting benefit was proven to be significant [5, 6]. However, wave farms are expected to generate current profiles far more variable than the ones produced by offshore wind farms. Under these conditions, the benefit of applying dynamic rating to these farms is therefore expected to be even more significant than in the case of wind farms. However, only few studies have focused on the techno-economic optimisation of wave farm electrical infrastructures, and, excluding the authors preliminary work [7],

This is an open access article under the terms of the [Creative Commons Attribution](https://creativecommons.org/licenses/by/4.0/) License, which permits use, distribution and reproduction in any medium, provided the original work is properly cited.

© 2021 The Authors. *IET Renewable Power Generation* published by John Wiley & Sons Ltd on behalf of The Institution of Engineering and Technology

none of them have addressed the exploitation of thermal inertia [8–10]. Hence, this paper proposes to address this question in the perspective of maximising the use of existing infrastructures.

This work considers a fictive, but assumed already existing wave energy test site. The number of wave energy converters (WECs) assumed to be integrated in this farm is assumed to comply with steady-state, electrical current constraints, that is the maximum current flowing through the export cable does not exceed its rated value. This approach is the one that is mostly applied nowadays and which is based on standards such as IEC 60287 [11, 12]. However, it may be envisaged that after some years of use, once design methods will have evolved in order to include dynamic rating, the site owner may be inclined to increase the number of WECs above the rated number in order to fully exploit its infrastructure, and therefore to increase its revenues. This raises the question of the profitability of such an approach: would it be profitable to add, as a second stage, more WECs to an already existing wave energy test site? A case study was carried out on this question and its results are described in this paper.

This raises also a second question regarding the type of models required to perform a techno-economic analysis, as different modelling approaches are available and provide different trade-offs in terms of precision and computing time. The computing time corresponding to each approach needs indeed to be evaluated carefully before starting the type of techno-economic analyses targeted in this paper, as they require long simulations over one year at least. In other words, the temperature of the export cable should be assessed over one year at least, which may lead to a prohibitive computing time with some highly-detailed models. Also, some approaches, such as the one described in IEC standard 60853 [13], were not developed with highly variable, long and non-cyclic current profiles in mind, such as the ones found in wave energy. Hence, it is necessary to assess the precision of each model and their burden in terms of computing time at a first stage, in order to select the most suitable one. In this perspective, a comparative analysis between several electrothermal models is performed in this paper.

The paper is organized as follows : Section 2 describes the different models used in this paper while Section 3 details the two case studies. The first case study focuses on a comparative analysis between several electrothermal models, and the second one on the techno-economic analysis mentioned earlier in this introduction. Then, Section 4 describes the results and Section 5 concludes the paper.

## 2 | METHODS

### 2.1 | Wave farm infrastructure and wave climate

The test site considered in our case studies is the French multi-technology, open sea test site “SEM-REV” operated by Ecole Centrale de Nantes [14]. This test site is located off Le Croisic, France and includes a 24 km-long submarine export cable, as



**FIGURE 1** Map of the SEM-REV test site. The continuous green and red lines represent the onshore connection, while the dotted green line represents the submarine export cable. Figure modified, courtesy of École Centrale de Nantes

shown in Figure 1. This cable is designed for a maximum temperature of 90 °C. Although exceeding this temperature may in practice lead to a negligible amount of additional aging, this may constitute a breach in insurance/guarantee contracts, thus rendering the test site owner potentially legally responsible in case cable failures, linked or not to this accelerated aging. Therefore, the possibility of exceeding the maximum allowed temperature of 90 °C will not be considered in this paper.

Time series of the significant wave height  $H_s$  (in m) and of the peak period  $T_p$  (in s) for this particular site, and at the temporal resolution of 30 min, were provided for this study. This data combines both on-site, buoy-measured data as well as re-simulated data using the HOMERE database [15]. The wave power spectral density is calculated based on these statistical indices ( $H_s$  and  $T_p$ ), and leads to an approximation of the real wave power encountered at this test site [16].

The sea-state time series were then used to simulate the sea level at 36 different locations, each representing the position of a potential wave energy converter. The sea level time series were then used as inputs in a wave-to-wire model of a passively-controlled, 1 MW-rated point absorber already described in a previous work [7]. This resulted in individual time series of the electrical power for each WEC, thus allowing to simulate the electrical power profile of a fictive wave farm including up to 36 WECs which could be installed in the vicinity of the SEM-REV test site. During each sea-state defined by a ( $H_s$ ,  $T_p$ ) couple, it was considered that the optimal damping factor maximising the energy conversion for the considered sea-state was applied to the WECs. Finally, electrical current time series were obtained by assuming that the wave farm would deliver power at a unity power factor under a phase-to-phase voltage of 20 kV.

### 2.2 | Cable electrothermal models

The thermal response of the submarine export cable to a given electrical current profile can be simulated by several types of electrothermal models, all presenting a different trade-off between computing speed and precision.

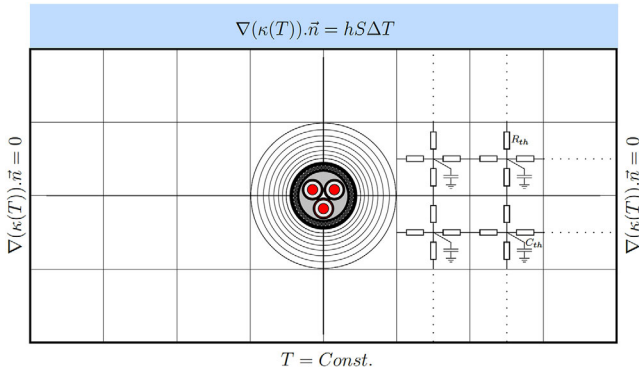


**FIGURE 2** Illustration of the discretisation of the cable and its direct environment, including the boundary conditions, as implemented under Matlab for the RC models (not to scale)

Finite element method (FEM) models have the capability to represent reality with a high level of accuracy, therefore leading to potentially very precise results. However, they are often quite computing time-hungry. So-called “RC” models, based on the thermal–electrical analogy, may present a dramatically reduced computing time for a potentially acceptable loss of precision. Last, but not least, simplified models, such as the ones proposed in IEC standards 60287 and 60853-2, may provide interesting results in a fraction of the computing time required by the other two types of models mentioned earlier. The objective of this section consists in detailing the different models (FEM, RC, IEC 60287 and 60853-2) which were analysed for the techno-economic analysis described later.

### 2.2.1 | Finite element method model

A 2D FEM model was developed under COMSOL and is detailed in a previous work [7]. It includes a strong coupling between the “heat transfer in solids” module (ht) and the “magnetic fields” module (mf). It should be emphasized that this model was validated against experimental simulations on a sample of the cable which is actually deployed at the SEM-REV test site. It will be used as the reference for the models comparative analysis.

### 2.2.2 | RC models

So-called “RC models” are based on the well-known thermal–electrical analogy [17]. In this paper, the cable and its environment were discretised in numerous elements containing thermal resistances and capacitances, as illustrated in Figure 2. The boundary conditions of the thermal problem are also defined in this figure.

The model was implemented in Matlab, and is based on the general heat equation:

$$\rho_m C_p(\theta) \frac{\partial \theta}{\partial t} = \nabla(\kappa(\theta) \nabla \theta) + \mathcal{Q}_j \quad (1)$$

where  $\rho_m$  is the mass density of each material and  $\kappa$  is the thermal conductivity taken from IEC standard 60287-2-1. The total Joule losses inside the cable are computed from the electrical model and defined by  $\mathcal{Q}_j = \int_V r_e J^2 dV$ , where  $J$  is the electric current density. The armour and screen losses were computed with respect to IEC standard 60287-1-1. Non-linear laws of cooling on the external boundaries were also used to model the heat transfer in sea water as:

$$\mathcal{Q}_c = b(\Delta\theta) \times S \times (\theta_w - \theta_s) \quad (2)$$

where  $\theta_s$  is the soil temperature of the RC element adjacent to the sea water,  $S$  is its area,  $\theta_w$  is the sea water temperature,  $b(\Delta\theta)$  is an effective non-linear convection coefficient expressed in  $W/(Km^2)$ , and  $\Delta\theta = \theta_w - \theta_s$ . Term  $b(\Delta\theta)$  is based on materials data and formulae given in IEC standards 60287, and is defined by the following equation:

$$b(\Delta\theta) = \frac{\kappa(\theta)}{L_c} \times 0.15 \times [Ra(\Delta\theta)]^{1/3} \quad (3)$$

where  $Ra(\Delta\theta)$  is the Rayleigh number which depends on the difference between the considered boundary temperature and the sea water temperature. It is defined as:

$$Ra(\Delta\theta) = \frac{g\beta\Delta\theta L_{cb}^3}{\nu\alpha_{th}} \quad (4)$$

where  $g$  is the acceleration due to gravity,  $\beta$  is the thermal expansion coefficient of the fluid,  $L_{cb}$  is the characteristic length,  $\nu$  is the kinematic viscosity and  $\alpha_{th}$  is the thermal diffusivity.

Three RC models were developed. The first one includes the relationships (sometimes highly non-linear) with temperature of the different materials thermal characteristics (resistance and capacitance) and will be referred to as “Model 1”. The second RC model includes only the linear relationship with temperature of the conductor thermal characteristics, while the other characteristics are supposed to be constant. This model will be referred to as “Model 2”. The last model, referred to as “Model 3”, is similar to Model 2, but transforms the input current profile into time series of 30-min RMS values, and computes the temperature profile based on this transformed time series. This is intended to reduce significantly the required computing time compared to Model 2.

### 2.2.3 | Model based on IEC standard 60287

According to IEC standard 60287-1-1, the conductor temperature  $\theta_c$  of a cable subjected to a constant current of RMS amplitude  $I$  can be expressed as:

$$\begin{aligned} \theta_c = & \theta_{amb} + (I^2 R + 0.5W_d)T_1 \\ & + [I^2 R(1 + \lambda_1) + W_d]nT_2 \\ & + [I^2 R(1 + \lambda_1 + \lambda_2) + W_d]n(T_3 + T_4) \end{aligned} \quad (5)$$

**TABLE 1** Numerical values of the parameters used for the models based on IEC standards 60287 and 60853

| Description                                          | Name                   | Numerical value              | Unit              |
|------------------------------------------------------|------------------------|------------------------------|-------------------|
| Thermal resistance (insulation)                      | $T_1$                  | 0.4749                       | K/W               |
| Thermal resistance (filler)                          | $T_2$                  | 0.2725                       | K/W               |
| Thermal resistance (internal sheath and armour mats) | $T_3$                  | 0.0455                       | K/W               |
| Thermal resistance (soil)                            | $T_4$                  | 0.4687                       | K/W               |
| Loss factors                                         | $\lambda_1, \lambda_2$ | 0, 0.0487                    |                   |
| Equivalent thermal resistances                       | $T_A, T_B$             | 0.1583, 0.3205               | K/W               |
| Thermal resistances                                  | $T_a, T_b$             | 0.0914, 0.3874               | K/W               |
| Factors                                              | $a, b$                 | 0.0104, $8.1 \times 10^{-4}$ | K/W               |
| Equivalent thermal capacitances                      | $Q_A, Q_B$             | 792.8, 2.950                 | J/K               |
| Soil diffusivity                                     | $\delta$               | $714 \times 10^{-9}$         | m <sup>2</sup> /s |
| Soil thermal resistivity                             | $\rho_e$               | 0.7                          | K m/W             |
| External cable diameter                              | $D_e$                  | 0.0893                       | m                 |
| Ambient temperature                                  | $\theta_{amb}$         | 12                           | °C                |
| Cable burial depth                                   | $L_c$                  | 1.5                          | m                 |

where  $\theta_{amb}$  is the ambient temperature,  $R$  the conductor resistance,  $W_d$  the dielectric losses,  $T_1$  to  $T_4$  the different thermal resistances composing the cable and the soil,  $\lambda_1$  and  $\lambda_2$  loss factors due to the induced currents in the screens and in the armour and  $n$  the number of conductors.

This standard has been generally used by grid operators and designers for cable sizing, based on the maximum current  $\max(I(t))$  that may flow through the cable, regardless of its potentially varying nature, and of the cable potentially significant inertia. Hence, this may lead to highly conservative estimates. In this paper, Equation (5) was used to calculate the maximum temperature that may be reached by the cable if it had no inertia, that is if steady-state conditions were achieved instantaneously. The results obtained with this model will be used as a worst-case reference in the models comparative analysis.

## 2.2.4 | Model based on IEC standard 60853

Contrary to IEC standard 60287, which was intended for constant current profiles and steady-state conditions, IEC standard 60853 details the procedure to simulate the transient thermal response  $\theta_c(t)$  of a cable subject to a potentially varying current profile, which is expressed as:

$$\theta_c(t) = \theta_{amb} + \theta_s(t) + \alpha(t)\theta_e(t) \quad (6)$$

where  $\theta_s(t)$  is the transient temperature rise above the ambient of the cable external surface,  $\theta_e(t)$  is the transient environmental temperature rise and  $\alpha(t)$  is the attainment factor. As the temperature is dependent on the Joule losses, themselves dependent on the temperature, the temperature is calculated iteratively by

re-updating the Joule losses once a new temperature is calculated, until the temperature reaches convergence.

Calculating the transient temperature rise of the cable external surface  $\theta_s(t)$  requires reducing the cable to a simple equivalent single-phase ladder thermal model, itself further reduced to a RC two-cell model including two thermal resistances  $T_A$  and  $T_B$ , as well as two capacitances  $Q_A$  and  $Q_B$ . The numerical values obtained for these parameters are listed in Table 1. Following this, the cable external surface transient response can be calculated as:

$$\Theta_c(t) = W \times [T_a(1 - e^{-at}) + T_b(1 - e^{-bt})] \quad (7)$$

where  $t$  is the time, and parameters  $a, b, T_a$  and  $T_b$  can be calculated based on the following formulae:

$$a = -x_2 \quad (8)$$

$$b = -x_1 \quad (9)$$

$$T_a = -T_{x_2} \quad (10)$$

$$T_b = -T_{x_1} \quad (11)$$

Terms  $x_1, x_2, T_{x_2}$  and  $T_{x_1}$  can be calculated as:

$$x_1 = -\frac{M_0}{N_0} + \frac{\sqrt{M_0^2 - N_0}}{N_0} \quad (12)$$

$$x_2 = -\frac{M_0}{N_0} - \frac{\sqrt{M_0^2 - N_0}}{N_0} \quad (13)$$

$$T_{x_1} = \frac{\frac{1}{Q_A} + (T_A + T_B)x_2}{x_1 - x_2} \quad (14)$$

$$T_{x_2} = \frac{\frac{1}{Q_A} + (T_A + T_B)x_1}{x_1 - x_2} \quad (15)$$

where

$$2 \times M_0 = Q_A \times (T_A + T_B) + Q_B \times T_B \quad (16)$$

$$N_0 = Q_A \times Q_B \times T_A \times T_B \quad (17)$$

As for the attainment factor  $\alpha(t)$ , it can be expressed as:

$$\alpha(t) = \frac{T_a \times (1 - e^{-at}) + T_b \times (1 - e^{-bt})}{T_A + T_B} \quad (18)$$

Finally, the environment transient response  $\theta_e(t)$  can be calculated as:

$$\theta_e(t) = W \times \frac{\rho_e}{4\pi} \left( -Ei \left( \frac{-D_e^2}{16 \times \delta \times t} \right) - \left( -Ei \left( \frac{-L_c^2}{\delta \times t} \right) \right) \right) \quad (19)$$

where  $W = 3R(I(t))^2(1 + \lambda_1 + \lambda_2)$  is the thermal flux generated by the three conductors,  $\rho_e$  is the soil thermal resistivity,  $\delta$  thermal diffusivity,  $L_c$  the cable burial depth and term  $Ei$  represents the integral exponential function.

### 2.3 | Economical models

As wave energy technology is still in its infancy, no wave farm has been deployed yet. Therefore, operational experience feedback and precise techno-economic data are unavailable. Hence, the data on which our techno-economic analysis is based relies on cost estimations described in a report by Sandia National Laboratories [18]. This report describes ‘‘Marine Energy Conversion reference models’’ for different types of WECs, and includes a comprehensive analysis of the different CAPEX and OPEX related to each model. Sandia’s estimations on point absorber costs were considered in this research work, where it was assumed that WECs were available on the market and that their production had reached an industrial production level, therefore leading to significant economies of scale. It should be emphasized that the techno-economic analysis proposed here is based on simple techno-economic models which may require to be refined by economists, especially once more realistic figures become available. It should also be noted that it was assumed

in this study that the farm electrical infrastructure (e.g. export cable, umbilicals, substations, etc.), being already existing, was already paid for, so its costs were not considered in this study: only the costs directly related to the additional WECs (including their transport, deployment and maintenance) were considered.

In order to assess whether the overplanting of WECs could be economically profitable, and if so, up to which number of additional WECs it would be profitable, the benefit  $B_A$  per additional WEC per year must be calculated as a function of the number of WECs for different feed-in tariffs. This benefit  $B_A$  can be expressed as:

$$B_A = R_A - C_A \quad (20)$$

where  $R_A$  is the annual revenue per additional WEC and  $C_A$  represents the annual expenses per additional WEC. Revenue  $R_A$  can be calculated as:

$$R_A = \frac{AEP \times FIT}{N_{WEC}^+} \quad (21)$$

where  $AEP$  is the annual energy production,  $FIT$  is the feed-in tariff, and  $N_{WEC}^+$  is the number of additional WECs. The annual cost  $C_A$  is obtained by summing all the costs over the wave farm lifetime (which was assumed to be equal to 20 years), divided by this lifetime. Some of the costs composing the annual costs  $C_A$  were provided in the Sandia report as total costs (i.e. over the wave farm lifetime) per kW. Hence, in order to calculate costs per WEC per year, they were multiplied by term  $C_{yr}$  which can be expressed as:

$$C_{yr} = \frac{D2E \times P_{WEC} \times in}{AMO} \quad (22)$$

where  $D2E$  is a US dollar to euro conversion rate,  $P_{WEC}$  corresponds to the rated power of a single WEC,  $in$  is the inflation rate between the publication year of the Sandia report (2014) and year 2019 (as the study was conducted in the course of 2020),  $AMO$  represents the amortisation period which is 20 years (i.e. the assumed lifetime of the wave farm). Term  $D2E$  was selected as the average conversion rate between 2014 and 2019, and is equal to 0.89 €//\$ [19]. Also, the inflation rate between 2014 and 2019 was considered, and estimated as equal to 5.2% [20].

The annual costs are composed of WEC structure costs  $M_{struc}$ , power conversion chain costs  $M_{PCC}$ , mooring costs  $M_{moor}$ , deployment and installation costs  $DI$ , operating, maintenance and monitoring costs  $OMM$ , such as:

$$C_A = M_{struc} + M_{PCC} + M_{moor} + DI + OMM \quad (23)$$

The equations defining each of these costs will now be described. The WEC structure costs can be defined as:

$$M_{struc} = C_{struc} C_{yr} \quad (24)$$

where  $C_{struc}$  is the cost of the WEC structure, which has been evaluated to 6070 \$/kW. Then, the power conversion chain costs  $M_{PCC}$ , related to the PTO, transformers, power converters, cables, etc. were calculated. As the considered type of WEC considered in this study is a direct-drive point absorber, costs related to hydrodynamic parts were excluded. This cost can be expressed as:

$$M_{PCC} = C_{PCC} C_{yr} \quad (25)$$

where  $C_{PCC}$  is the cost of the whole power conversion chain, which has been evaluated to 1110 \$/kW. The manufacturing costs of the moorings, and the associated buoyancy and anchoring system,  $M_{moor}$  can be expressed as:

$$M_{moor} = C_{moor} C_{yr} \quad (26)$$

where  $C_{moor}$  has been evaluated to 1651 \$/kW. The deployment and installation costs ( $DI$ ) of both the additional WECs and of their mooring systems is defined as:

$$DI = CI(N_{WEC}^+) C_{yr} \quad (27)$$

where  $CI$  is the cost of installation in \$/kW that is highly dependent on the number of additional WECs  $N_{WEC}^+$ , and was evaluated to approximately 1500 \$/kW. Term  $N_{WEC}^+$  is the total number of WECs minus the number of WECs (Equation (11)) in the base case where current constraints are considered. Finally, the operating, maintenance and monitoring annual costs  $OMM$  must be calculated. This term depends on the total number of WECs  $N_{WEC}^{tot}$  that are installed in the farm, and can be expressed as:

$$OMM = C_{OMM}(N_{WEC}^{tot}) \times D2E \times P_{WEC} \times in \quad (28)$$

where  $C_{OMM}$  was evaluated to  $\approx 300$  \$/kW.

### 3 | CASE STUDIES

In each of the two case studies, the ambient temperature of the soil and the sea water was assumed to be equal to 12 °C, which is typical of northwestern European coastal conditions, as defined in Berx and Hughes [21]. Simulations were performed assuming that the export cable is buried at a constant depth of 1.5 m under the sea bed. It is assumed that the wave farm includes 11 WECs, leading to a maximum current close to, but not exceeding, the cable rated current equal to 330 A.

#### 3.1 | Comparative analysis on the electrothermal models

In order to perform a comparative analysis of the different electrothermal models, a relatively short period of time was considered, thus leading to reasonable computing times, even for

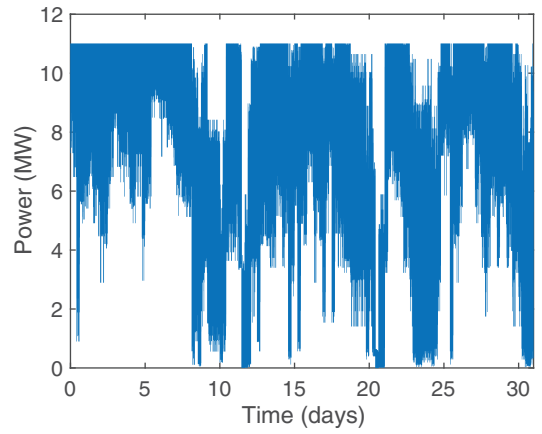


FIGURE 3 Power profile of the wave farm (1st January–31st January, 2015) used for the comparative analysis of the electrothermal models

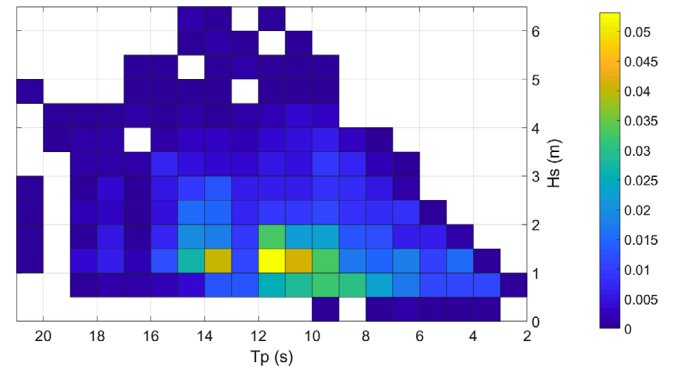


FIGURE 4 Scatter matrix of the SEM-REV wave resource showing the sea-state occurrence ratio (between 0 and 1) over the 12-month period considered in this paper (June 2014 to June 2015)

the FEM model which is the most computing time-demanding. The period considered in this case study spans between January 1, 2015 and January 31, 2015. The corresponding power profile is shown in Figure 3. This period was selected as constituting the most energetic window over a 12-month period spanning between June 2014 and June 2015, this latter period being retained for the techno-economical analysis.

#### 3.2 | Techno-economical analysis

As mentioned earlier, the techno-economical analysis was performed based on a wave farm power profile simulated for June 2014 to June 2015. The scatter matrix corresponding to this period is shown in Figure 4. Based on the observations that will be detailed in Section 4, RC Model 3 was decided to be used for performing this study as it presents a reasonable trade-off between precision and computing time.

In this study, the number of WECs is allowed to vary every 30 min. In other words, curtailment is allowed as WECs can be switched on or off, in order to maximize the electricity generation while satisfying the cable temperature constraints.

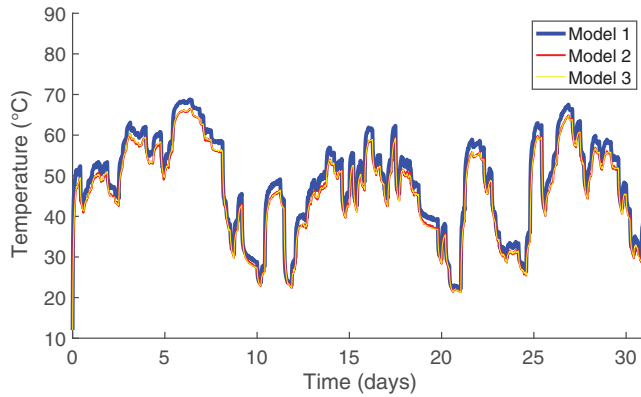


**FIGURE 5** Temperature profile over January 2015 as calculated with the three different RC models: Model 1 (non-linear thermal characteristics), Model 2 (constant thermal characteristics, except for the linear relationship with temperature of the conductor material), Model 3 (similar to Model 2, but transforming the electrical current input profile into 30-min RMS time series before calculating the corresponding temperature)

A simple strategy was used to calculate the electricity generation at each time step of 30 min. First, a given number of additional WECs  $N_{WEC}^+$  was considered. A simulation was performed to determine whether the cable temperature exceeded the maximum allowed temperature of 90 °C. When that was the case, the considered number of WECs was reduced iteratively by one WEC, until the cable temperature constraints was satisfied. The highest number of WECs obtained through this method was then retained to calculate the energy generation for the considered 30 min-time step, while the total costs were calculated based on the additional number of WECs  $N_{WEC}^+$  (whether they generate electricity or not). This allowed to simulate the potential curtailment of some WECs, thus allowing a variable number of WECs to generate electricity as a function of time in order to maximise the energy harvesting while satisfying thermal constraints. A maximum number of WECs  $N + WEC$  equal to 36 was considered. For the sake of comparison, the study was also conducted for a fixed number of WECs  $N + WEC$  ranging between 11 WECs and 13 WECs.

## 4 | RESULTS AND DISCUSSION

### 4.1 | Comparative analysis on the electrothermal models

The temperature profiles for the three different RC models described in Section 2 are shown in Figure 5. In terms of maximum temperature, Model 1 reaches 68.8 °C, while Models 2 and 3 reach both 66.5 °C, thus leading to an acceptable loss of precision of 2.3 °C. Regarding the entire temperature profiles, it can be observed that the curves of Models 2 and 3 are superimposed. This means that simplifying the input electrical current profile by considering only its 30-min RMS time series is sufficient. It can also be observed that the error between Model 1 and Models 2 and 3 is relatively negligible, whereas Model 1 is

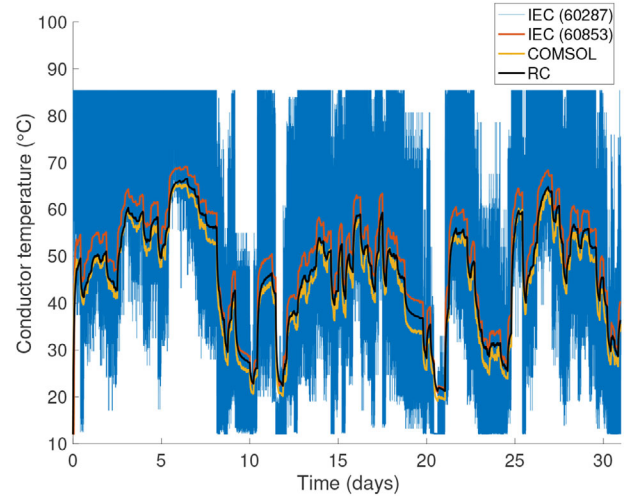


**FIGURE 6** Temperature profiles over January 2015 for the FEM model (“COMSOL”), RC Model 3 (“RC”), and models based on IEC standards 60853 (“IEC 60853”) and 60287 (“IEC 60287”)

more time computing-hungry than Model 2 and far more time computing-hungry than Model 3.

Figure 6 shows the temperature profile for a period spanning over January 2015 for four different models: the FEM model developed under COMSOL, two models based on IEC standards 60287 and 60853 respectively, and RC Model 3, referred to as “RC” in this figure, for the sake of simplicity.

The model based on IEC standard 60287 shows a maximum temperature equal to 85 °C, which is slightly below the maximum allowed temperature of 90 °C. This is explained by the fact that the wave farm is assumed to include 11 WECs, whose maximum aggregated current is slightly below the maximum allowed current. This choice was done as including 12 WECs permanently in the wave farm would have led to a maximum current exceeding the cable rated current equal to 330 A.

The difference between the steady-state model based on IEC standard 60287, which implicitly does not include the effect of thermal inertia, and the other models is extremely important. It can indeed be observed that the maximum temperature with the IEC standard 60287-based model is equal to 85 °C whereas the maximum temperature observed for the FEM model, Model 3 (RC model) and IEC standard 60853-based model are equal to 65, 66, and 69 °C, respectively. This highlights that there may be a very significant benefit in exploiting the thermal inertia of the submarine cable, as the effect of thermal inertia is very important. It can also be observed that RC Model 3 performs quite well compared to the FEM model, while requiring only a fraction of the latter’s computing time. The computing time for all the different models is detailed in Table 2. These computing times correspond to a simulation of 7 days at a time step of 10 seconds. The computations were performed on a computer having a 4 cores, Intel Xeon W-2125 processor with a base frequency of 4.0 GHz. However, the results obtained from the model based on IEC standard 60853 show that this standard is quite conservative, as it over-estimates the temperature by 4 °C, which is quite significant. Hence, selecting RC Model 3



**TABLE 2** Computing time for the different electro-thermal models

| Model                      | Computing time |
|----------------------------|----------------|
| FEM COMSOL                 | 26 h 44 m      |
| Model 1                    | 8 h 46 m       |
| Models 2 and 3 (RC models) | 28 m 40 s      |
| IEC 60853                  | 16 m 57 s      |

**TABLE 3** Additional annual energy production (AEP) compared to the best case with 11 WECs, ratio between the maximum current  $\max(I(t))$  and the rated current  $I_r=330$  A, and maximum temperature for different WEC numbers with (Y) and without (N) curtailment allowed

| WEC number | Curtailment allowed (Y/N) | Add. AEP per add. WEC (MWh) | Ratio max $(I(t))/I_r$ | Max. temperature ( $^{\circ}$ C) |
|------------|---------------------------|-----------------------------|------------------------|----------------------------------|
| 11         | N                         | 0                           | 0.96                   | 68.5                             |
| 12         | N                         | 3667                        | 1.05                   | 81.8                             |
| 13         | N                         | 3607                        | 1.14                   | 97.8                             |
| 11 to 13   | Y                         | 3536                        | 1.14                   | 90                               |
| 11 to 14   | Y                         | 3091                        | 1.22                   | 90                               |
| 11 to 15   | Y                         | 2435                        | 1.31                   | 90                               |
| 11 to 16   | Y                         | 1923                        | 1.40                   | 90                               |
| 11 to 36   | Y                         | 771                         | 2.87                   | 90                               |

for performing the techno-economic analysis, whose results are described in the next section, was decided to represent the most reasonable trade-off between required computing time and precision.

## 4.2 | Techno-economical analysis

The objective of the techno-economical analysis was to determine under which conditions in terms of additional number of WECs and of feed-in tariffs adding WECs to an existing test site could be profitable while satisfying the cable electrothermal constraints.

Table 3 shows the additional annual energy production (with respect to the base case with 11 WECs), the maximum temperature, and the ratio between the maximum current and the rated current of 330 A for several number of WECs, with and without curtailment. It can be observed that adding permanently 2 WECs without allowing curtailment (i.e. reaching a number of 13 WECs where curtailment would not be allowed) would lead the cable temperature to exceed its maximum allowed limit of 90  $^{\circ}$ C. However, a significant amount of energy can be harvested by adding more WECs while allowing curtailment. Of course, the higher the number of WECs, the less amount of electricity per WEC can be generated as curtailment is applied more and more regularly. This means that the benefit per WEC is expected to increase at first, and then decrease with the number of WECs.

Figure 7 shows the benefit  $B_A$  (in k $\text{€}$  per additional WEC and per year) as a function of the additional number of WECs  $N_{WEC}^+$  and for different feed-in tariffs  $FIT$ .

In the cases where benefit  $B_A$  is positive, it can be observed that the optimum benefit is found for the addition of only two WECs. This is explained by the fact that the higher the number of WECs, the more often the added WECs would have to be curtailed to prevent the cable temperature from exceeding 90  $^{\circ}$ C. Therefore, the revenue per WEC is expected to decrease with the increase of the WEC number, which is observed here.

It can also be observed that a positive benefit (i.e. meaning a revenue greater than the expenses) is observed only from high feed-in tariffs greater than 700 $\text{€}/\text{MWh}$ . It is interesting to note that feed-in tariffs around the world for renewables and in particular for wave energy, are within a range of 200 to 600  $\text{€}/\text{MWh}$  [22, 23]. The results obtained in this analysis show therefore that it would not be profitable to envisage adding WECs to the existing test site considered in this study. This result can be explained by several factors. First of all, the SEM-REV test site presents a relatively mild wave climate compared to other sites in the world. Its annual average power is indeed equal to 12 kW/m only while the Portuguese pilot zone reaches 32 kW/m, and Belmullet in Ireland shows an average wave power of nearly 70 kW/m [24, 25]. However, in the absence of data from these other sites, the SEM-REV was retained as a worst-case scenario from a wave climate perspective. Also, the considered test site is rated to a relatively low level ( $\approx 10$  MW), which means that increasing the maximum power of the farm by few tens of percent would lead to adding only few WECs. Hence, costs such as transport, which represents a heavy share of the total costs, are borne by these few WECs only, therefore increasing dramatically the costs per WEC. In a farm rated to a higher power level, for example a pre-commercial wave farm of few tens of MW, the transport costs could be shared among more WECs, therefore leading to reduced per WEC costs. In this perspective again, considering the SEM-REV test site also constitutes a worst-case scenario. However, the additional costs linked to the upgrading of the substations, cable junctions, and of the landfall section were not considered. These sections present a less important, but still significant, inertia than the buried part of the submarine cable, and may therefore need to be modified if the maximum allowed power of the test site were increased. However, this may require a more in-depth analysis, as these pieces of equipment may also benefit from natural cooling in winter times when wave energy is more abundant, while in summer times, where heating due to solar radiation is more important, wave energy production may be at a minimum.

Based on these observations, it may be concluded that adding WECs to an existing test site is not profitable under the current conditions due to the still very high cost of wave energy technology. As these costs are expected to decrease in the future, this analysis will have to be updated accordingly. The results also show that, although the envisaged perspective is not profitable under the conditions considered here, it is close to the limit for profitability with the highest feed-in tariffs values. Therefore, a

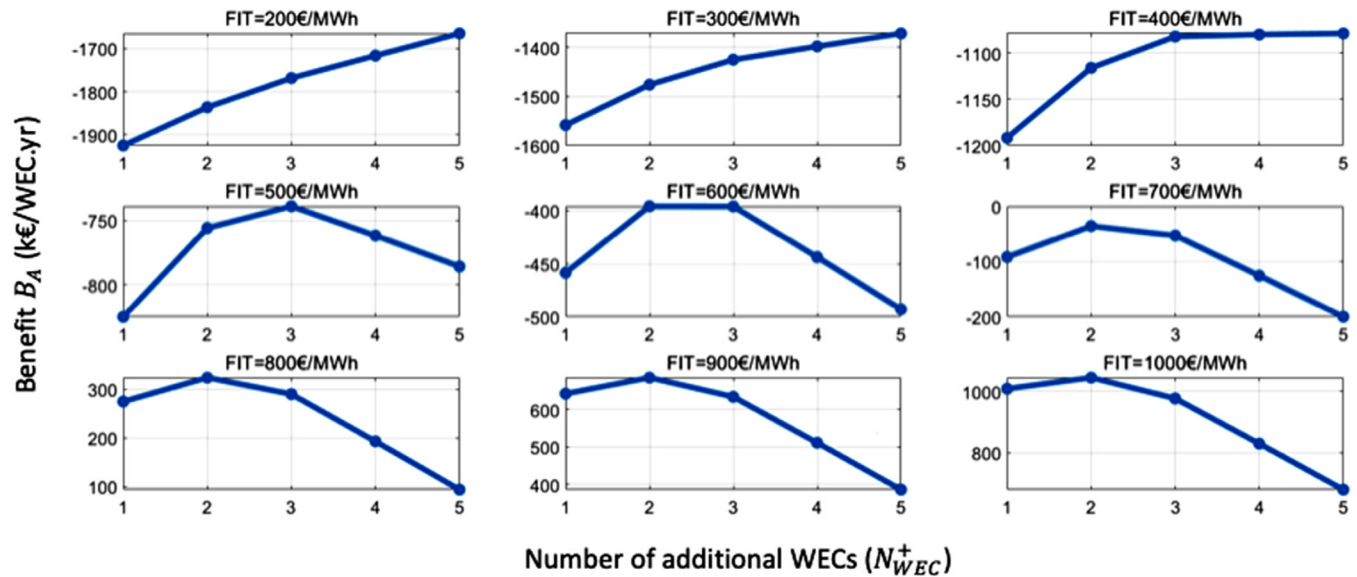


FIGURE 7 Benefit  $B_A$  in k€ per additional WEC and per year as a function of the additional number of WECs  $N_{WEC}^+$  and for different feed-in tariffs  $FIT$

more detailed analysis would be required to determine whether adding WECs to more energetic test sites, and/or presenting a higher rated power, could be profitable. However, it is clear that a single-stage approach, were dynamic rating is considered initially in the design of the farm, rather than after its deployment, would be more economically competitive, as dividing the deployment of the farm into two steps may jeopardize the economic benefit of exploiting thermal inertia.

## 5 | CONCLUSIONS

This paper described two case studies on the grid integration of wave energy in the perspective of exploiting the thermal inertia of a wave farm submarine cable. In the first case study, a comparative analysis of different cable electrothermal models was performed. The most precise model, based on the finite element method (FEM) and validated experimentally, was used as a benchmark for the other models. It was shown that using an RC model with constant thermal characteristics, except for the conductors ones, and based on 30 min-RMS input data (referred to “Model 3”), led to relatively precise results. However, it was shown as well that the model based on the IEC standard 60853 was quite conservative, as a difference in terms of maximum temperature of 4 °C was found. This represents more than 4% of the maximum allowed temperature of 90 °C and can be considered as significant. Hence, RC Model 3 was used to perform a techno-economic analysis involving the simulations of wave energy generation over 1 full year at the time step of 30 min. It was concluded that, under the conditions considered in this study, which may represent worst-case conditions in terms of rated power and wave climate, it is not profitable to install additional WECs at a test site as a second stage, given the still quite high expected levelized cost of wave energy. However, this may not be the case for more energetic test sites and/or presenting a higher rated power. Hence, more detailed analyses are required

to determine whether adding additional WECs to such an existing test site could be profitable. Also, it was recommended to include dynamic rating at the initial design stage of the wave farm, as considering it after the deployment of the farm may jeopardize its potential economic benefit.

## ACKNOWLEDGMENTS

This research work was conducted as part of the “BlueGrid” project funded by the Brittany Regional Council and ENS Rennes, and the “ORIGAMI” and “CELT4Wind” projects carried out within the framework of the WEAMEC, West Atlantic Marine Energy Community, and with funding from the CARENE and the Pays de la Loire Region. All these organisations are gratefully acknowledged.

## ORCID

Anne Blavette  <https://orcid.org/0000-0002-2911-3178>

## REFERENCES

1. RTE: Grandes lignes du programme de R&D de RTE sur la période 2017–2020, Technical report, (2017) <https://www.cre.fr/content/download/16299/202068> Accessed May 25, 2021
2. Foss, S.D., Maraió, R.A.: Dynamic line rating in the operating environment. *IEEE Trans. Power Delivery* 5(2), 1095–1105 (1990)
3. Daminov, I. et al.: Receding horizon algorithm for dynamic transformer rating and its application for real-time economic dispatch. In: *IEEE Milan PowerTech*, Milan, Italy (2019), pp. 1–6
4. Viafora, N., et al.: Day-ahead dispatch optimization with dynamic thermal rating of transformers and overhead lines. *Electr. Power Syst. Res.* 171, 194–208 (2019)
5. Catmull, S. et al.: Cyclic load profiles for offshore wind farm cable rating. *IEEE Trans. Power Delivery* 31(3), (2016)
6. Perez-Rua, J.A., Cutululis, N.A.: Electrical cable optimization in offshore wind farms—a review. *IEEE Access* 7, 85796–85811 (2019)
7. Bonnard, C.H., et al.: Modeling of a wave farm export cable for electrothermal sizing studies. *Renewable Energy* 147, 2387–2398 (2020)
8. Sharkey, F., et al.: Maximising value of electrical networks for wave energy converter arrays. *Int. J. Mar. Energy* 1, 55–69 (2013)

9. Bull, D., Baca, M., Schenkman, B.: Electrical cable utilization for wave energy converters. *J. Ocean. Eng. Mar. Energy* 4(2), 171–186 (2018)
10. Nambiar, A. et al.: Optimising network design options for marine energy converter farms. In: 11th European Wave and Tidal Energy Conference EWTEC, Nantes, France (2015)
11. IEC 60287-1-1: Electric cables - Calculation of the current rating - Part 1-1: Current rating equations (100 % load factor) and calculation of losses - General. (2006)
12. IEC 60287-2-1: Electric cables - Calculation of the current rating - Part 2-1: Thermal resistance - Calculation of thermal resistance. (2006)
13. IEC 60853-2: Calculations of the cyclic and emergency current rating of cables. Part 2 : cyclic rating of cables greater than 18/30 (36) kV and emergency ratings for cables of ALL voltages. (1989)
14. SEM-REV, <https://sem-rev.ec-nantes.fr/>. Accessed May 25, 2021
15. HOMERE database, <https://sextant.ifremer.fr/record/cf47e08d-1455-4254-955e-d66225c9dc90/>, <https://doi.org/10.12770/cf47e08d-1455-4254-955e-d66225c9dc90>. Accessed May 25, 2021
16. Pérignon, Y.: Assessing accuracy in the estimation of spectral content in wave energy resource on the French Atlantic test site SEM-REV. *Renewable Energy* 114(Part A), 145–153 (2017)
17. Robertson, A., Gross, D.: An electrical-analog method for transient heat-flow analysis. *J. Res. Nat. Bur. Stand.* 61(2), 105 (1958)
18. Neary, V.S. et al.: Report SAND2014-9040, Methodology for Design and Economic Analysis of Marine Energy Conversion (MEC) Technologies. Sandia National Lab.(SNLNM), Albuquerque, NM (United States) (2014) <https://energy.sandia.gov/wp-content/gallery/uploads/SAND2014-9040-RMP-REPORT.pdf>. Accessed January, 15, 2019
19. Internal Revenue Service of the United States, <https://www.irs.gov/>. Accessed May 25, 2021
20. Global Rates, Inflation France, <https://fr.globalrates.com/>
21. Berx, B., Hughes, S. L.: Climatology of surface and near-bed temperature and salinity on the north-west European continental shelf for 1971-2000. *Cont. Shelf Res.* 29(19), 2286–2292 (2009)
22. Chozas, J.F., Kofoed, J.P., Jensen, N.E.H.: User Guide–COE Calculation Tool for Wave Energy Converters. Aalborg University, Denmark (2014)
23. Ocean Energy Systems: An Overview of Ocean Energy Activities in 2018. Annual Report. <https://report2018.ocean-energysystems.org/documents/OES-Annual-Report-2018/>. Accessed May 25, 2021
24. Sheng, W., Lewis, T.: Energy conversion: A comparison of fix- and self-referenced wave energy converters. *Energies* 9(12), (2016)
25. Mora-Figueroa, V.O. et al.: Catalogue of wave energy test centres. Technical report. March (2011) [https://tethys.pnnl.gov/sites/default/files/publications/D2.1\\_Catalogue\\_of\\_Wave\\_Energy\\_Test\\_Centres.pdf](https://tethys.pnnl.gov/sites/default/files/publications/D2.1_Catalogue_of_Wave_Energy_Test_Centres.pdf). Accessed May 25, 2021

**How to cite this article:** Blavette, A. et al.: Upgrading wave energy test sites by including overplanting: a techno-economic analysis. *IET Renew. Power Gener.* 1–10 (2021). <https://doi.org/10.1049/rpg2.12220>